

about 2×10^9 to 3×10^9 . (Larger values for k_1 were not considered since, as discussed above, even 2×10^9 was considered surprisingly large.) Our simulations suggest that k_1 is a factor of 5 to 7 greater than k_e ($\sim 1.4 \times 10^{10}$). Thus the problem is no longer to understand why k_e is so large but rather to understand why it is so small.

The answer lies in the factor $k_2/(k_{-1} + k_2)$, which is just the probability of reacting once the substrate has associated with the active site. This probability approaches 1 if ($k_2 \gg k_{-1}$) (diffusion-limited). Our calculations suggest that the reaction probability is about 0.2 and that k_{-1} is therefore comparable in magnitude to k_2 . Turnover rates for SOD have been measured under saturation conditions at low temperature (17) and k_2 was found to be about 10^6 sec^{-1} . If we assume a reaction probability of 0.2, k_{-1} would be about $4 \times 10^6 \text{ sec}^{-1}$.

A low reaction possibility could result from (i) the difficulty of accessing the copper because of bound water (5, 6, 18), competition from bound anions attracted by the positive potential (19), or the narrow channel at the bottom of the active site, or (ii) slow diffusion of protons to the active site or slow dissociation of the product OH^- from the enzyme, both of which occur against the potential gradient.

Superoxide dismutase might be engi-

neered to increase the enzyme rate (i) by increasing k_1 with the addition of positive charge near the active site channel, or (ii) by increasing k_2 , which could increase the reaction probability by up to a factor of 5 to a value of unity. Increasing k_2 may be more difficult since the factors that influence it may be inherent properties of the active site channel. Perhaps the most striking conclusion from the results in Table 2 is that a complex protein such as SOD appears to mimic the effects of isolated cupric ions. The burial of the copper atom in the protein is offset by the focusing of the positive potential further out from the active site cleft into the solution due to the shape of the protein and its low dielectric constant. The charge distribution of the protein and its shape result in a quadropole-shaped electrostatic potential profile (8). The negative potential regions have no net effect on the association rate, whereas the positive regions, which are accessible to superoxide, provide a large collision surface and attract the ion efficiently to the copper atom.

The study of association of more complex substrates, protein-protein association (13) and protein-nucleic acid association, although computationally more demanding, is now within the realm of possibility by using extensions of the techniques described in this report.

REFERENCES AND NOTES

1. A. Fersht, *Enzyme Structure and Mechanism* (Freeman, New York, 1985).
2. D. Klug, J. Rabani, I. Fridovich, *J. Biol. Chem.* **247**, 4839 (1972).
3. A. Cudd and I. Fridovich, *ibid.* **257**, 11443 (1982).
4. W. H. Koppenol, in *Oxygen and Oxy-Radicals in Chemistry and Biology*, M. A. Rodgers and E. L. Powers, Eds. (Academic Press, New York, 1981), p. 671.
5. J. A. Tainer, E. D. Getzoff, K. M. Beem, J. S. Richardson, D. C. Richardson, *J. Mol. Biol.* **160**, 181 (1982).
6. J. A. Tainer, E. D. Getzoff, J. S. Richardson, D. C. Richardson, *Nature (London)* **306**, 284 (1983).
7. E. D. Getzoff *et al.*, *ibid.*, p. 287.
8. I. Klapper, R. Hagstrom, R. M. Fine, K. A. Sharp, B. Honig, *Proteins* **1**, 47 (1986).
9. K. A. Sharp, R. M. Fine, K. Schulten, B. Honig, *J. Phys. Chem.*, in press.
10. S. A. Allison, S. H. Northrup, J. A. McCammon, *Biophys. J.* **49**, 167 (1986).
11. S. A. Allison and J. A. McCammon, *J. Phys. Chem.* **89**, 1072 (1985).
12. S. H. Northrup, S. A. Allison, J. A. McCammon, *J. Chem. Phys.* **80**, 1517 (1984).
13. S. H. Northrup, J. C. Reynolds, C. M. Miller, K. J. Forest, J. O. Boles, *J. Am. Chem. Soc.* **108**, 8162 (1986).
14. G. Ganti, J. A. McCammon, S. A. Allison, *J. Phys. Chem.* **89**, 3899 (1985).
15. J. Stein, J. P. Fackler, G. J. McClune, J. A. Fee, L. T. Chan, *Inorg. Chem.* **18**, 3511 (1978).
16. D. Barra *et al.*, *FEBS Lett.* **120**, 53 (1980).
17. J. A. Fee and C. Bull, *J. Biol. Chem.* **261**, 13000 (1986).
18. R. Osman and H. Basch, *J. Am. Chem. Soc.* **106**, 5710 (1984).
19. C. Bull and J. A. Fee, *ibid.* **107**, 3295 (1985).
20. I. Fridovich, personal communication.
21. Supported by ONR grant N00014-86-K-0483 and NIH grant GM30518.

22 December 1986; accepted 13 April 1987

A New Method for Analyzing Powder Diffraction Patterns: Confirmation of a Predicted Phase of SF_6

LAWRENCE S. BARTELL, JACQUES C. CAILLAT, BRIAN M. POWELL

A recent computer simulation reproduced all of the solid-state transitions known for sulfur hexafluoride and predicted the unknown structure of its coldest phase. Subsequent neutron diffraction experiments that were performed to establish the structure of this phase could not be interpreted by conventional procedures. A method for analyzing Debye-Scherrer diffraction patterns was designed to avoid the many false minima that are encountered in standard analyses of low-symmetry phases. The structure found with this method confirmed the previous theoretical prediction.

CONSIDERABLE PROGRESS TOWARD understanding the structural and thermodynamic behavior of molecular solids was made several years ago in the molecular dynamics computer simulations of the sulfur hexafluoride (SF_6) system by Pawley and co-workers (1, 2). Although the octahedral SF_6 molecules are simple and quasi-spherical, the system is complex. Between its sublimation point (223 K) and 96 K, SF_6 exists in a body-centered cubic (bcc), plastic-crystalline phase (3). Under certain conditions it undergoes a transition to a trigonal structure when cooled below 96 K

(4). At still lower temperatures it transforms into a phase whose symmetry is no higher than monoclinic (4). Molecular dynamics computations by Pawley and co-workers (1, 2) with a sample of 4096 molecules demonstrated the existence of all three phases. They reproduced the known lattice constants for the two higher temperature phases and the spontaneous transitions as the temperature was lowered.

For the coldest phase the computations predicted an uncommon packing arrangement, namely, a triclinic lattice (space group $P1$), with three molecules per cell. The

prediction prompted an investigation of cold SF_6 in which neutron diffraction techniques were used. Because large single crystals could not be grown, measurements were made on polycrystalline samples in the low-temperature phase. Analysis of the crystal structure by conventional procedures proved intractable. Despite the examination of many thousands of sets of initial molecular configurations, no satisfactory unit cell was found in the subsequent refinements, so it was impossible to confirm or refute the predictions of Pawley and co-workers.

In concurrent research (5), submicroscopic crystals of SeF_6 and TeF_6 were obtained by homogeneous nucleation in their vapor phases in supersonic flow. To determine the lattice parameters of the microcrystals by electron diffraction, a procedure of analysis, documented in detail elsewhere (6), was devised. As a critical test the procedure was applied to the neutron data for SF_6 , and an

L. S. Bartell and J. C. Caillat, Department of Chemistry, University of Michigan, Ann Arbor, MI 48109.
B. M. Powell, Neutron and Solid State Physics Branch, Atomic Energy of Canada, Ltd., Chalk River Nuclear Laboratories, Chalk River, Ontario K0J 1J0, Canada.

excellent fit of the observed diffraction pattern was quickly obtained.

A polycrystalline sample of SF₆ was prepared by cryogrinding the condensed solid in a thin-walled sample container of vanadium (1.2 cm in diameter, 7 cm long). Diffraction patterns were recorded on the C5 triple-axis spectrometer, which operated in its two-axis mode at the NRU reactor, Chalk River, with a neutron wavelength λ of 1.8339 Å. Experimental profiles were measured by increasing the angle of the detector in intervals of 0.1° from 10° to 83°. Profiles of the cold phase were recorded at 23 and 75 K.

The procedure devised to determine the lattice constants had two stages: (i) generation of a reasonable trial model of the molecular packing and (ii) a previously untried approach to avoid entrapment in false minima during refinement of cell constants. Because the procedure is not based simply on peak positions but is a least squares minimization of the difference between experimental and calculated intensity profiles, the first stage is needed for the computation of approximate structure factors. To estimate atomic positions in the solid, a plausible representation of intermolecular energies was constructed by associating with each intermolecular atom-atom interaction a Buckingham potential energy function. Such functions consist of a repulsive component $B \exp(-Cr)$ and an attractive component $-Ar^{-6}$ expressing the interaction energy between any given pair of atoms (F ··· F, F ··· S, or S ··· S) separated by the distance r . The parameters adopted are listed in Table 1. These interactions were introduced into the program PCK6 designed by Williams (7) to minimize crystal-packing energy with respect to molecular positions. When the structure was constrained to be bcc, a lattice parameter of 5.74 Å was obtained. This value was close enough to the experimental value of 5.78 Å at 96 K (4, 5) to justify adopting the potential function in searches for additional minima that correspond to low crystal symmetry. Although such a simplified, ad hoc force field cannot be relied upon to yield precise structures and energies, its results should be useful as starting values for refinements of experimental crys-

tal data. For other types of systems, alternative model-building techniques might be more appropriate.

When the bcc structure was altered by rotating one-third of the molecules by 60° before minimization, as suggested by Raynerd *et al.* (4), an energy minimum that was 10 percent lower than the bcc minimum was found, and the structure corresponded to the intermediate trigonal phase. When the crystal symmetry was reduced to triclinic, two alternative minima were found, the deeper of which was comparable to that of the trigonal form. This solution indicated a splitting of the diffraction peaks in reasonable agreement with the observations. Furthermore, the PCK6 results for the lattice parameters (where a , b , and c are in angstroms and α , β , and γ are in degrees)

$$(a, b, c) = (14.10, 7.75, 4.67)$$

$$(\alpha, \beta, \gamma) = (88.8, 91.45, 88.1)$$

closely matched those of Pawley and Thomas (1),

$$(a, b, c) = (14.1, 7.7, 4.70)$$

$$(\alpha, \beta, \gamma) = (89.4, 91.9, 88.1)$$

which were based on a different (and to us, unknown) potential function. The method of Pawley and Thomas (1) can, in principle, realistically model the thermodynamic influence of temperature, whereas our energy minimizations cannot.

The strategy that we used to avoid becoming trapped in false minima in the least squares refinements of cell parameters was extremely simple, yet effective. False minima were "blurred" into a background that sloped gently toward the global minimum in the optimizations. This was done by initially including only a few of the innermost diffraction peaks and by broadening both the experimental and theoretical peaks according to an elementary prescription (6). This broadening ensured a sufficient overlap between corresponding experimental and theoretical features to allow the refinement to advance in the proper direction. When the low-angle peaks were well fitted, the angular range was increased and the broadening reduced, in stages, until the entire pattern was well represented.

An outline of the procedure is as follows. A table of "broadened" intensities $I_B^{\text{obs}}(S_i)$ was obtained from the original experimental intensities $I(S_i)$ by the expression

$$I_B^{\text{obs}}(S_i) = \sum_n \frac{\exp[-(n\Delta S)^2/2\sigma_B^2]}{(2\pi\sigma_B^2)^{1/2}} \cdot I(S_i - n\Delta S)\Delta S \quad (1)$$

in which the summation was from $-n_m$ to $+n_m$, with $n_m = 5\sigma_B/\Delta S$, and with ΔS de-

noting the interval of tabulation. Blurring was thus controlled by the parameter σ_B . The scattering variable for scattering angle $2\theta_i$ is S_i . The corresponding function $I^{\text{calc}}(S_i)$ representing scattered intensities of neutrons is given by

$$I^{\text{calc}}(S_i) = \sum_k K_k \exp[-(S_i - S_k)^2/2\sigma_E^2] \quad (2)$$

where the summation is over all Debye-Scherrer peaks k that contribute to the intensity at S_i . The factor K_k is determined by the multiplicity, the structure factor, and the natural width of the reflection k . Broadening of the calculated intensities $I^{\text{calc}}(S_i)$ is accomplished by replacing the experimental variance σ_E^2 by $\sigma^2 = \sigma_B^2 + \sigma_E^2$. The function to be minimized by a least squares procedure is then

$$y = \sum_i [I^{\text{obs}}(S_i) - I^{\text{calc}}(S_i)]^2 \quad (3)$$

Only the lattice parameters were refined in the current version of the program. In refinements to date, Debye-Waller thermal factors were adjusted only by inspection and not by true optimization. Final cell constants were, for the data at 23 K,

$$(a, b, c) = (14.040, 8.009, 4.749)$$

$$(\alpha, \beta, \gamma) = (85.21, 92.74, 89.11)$$

and for the data at 75 K,

$$(a, b, c) = (14.153, 8.079, 4.799)$$

$$(\alpha, \beta, \gamma) = (85.55, 92.54, 89.29)$$

Calculated intensities at 75 K are compared with experimental values in Fig. 1.

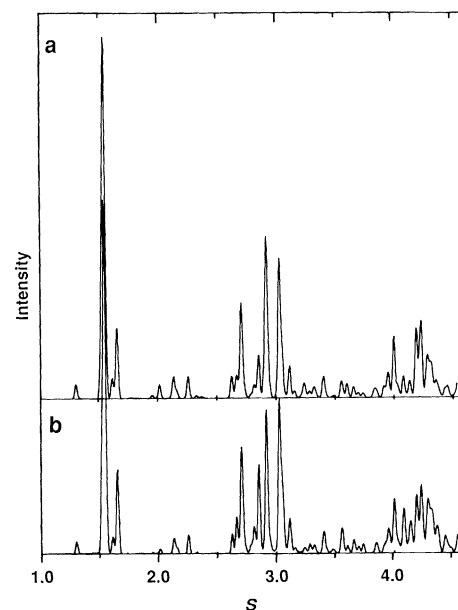


Fig. 1. Neutron diffraction patterns of polycrystalline SF₆ at 75 K: (a) calculated, (b) observed. $S = 4\pi \sin \theta/\lambda$.

Table 1. Parameters for intermolecular potential energy functions for SF₆ ··· SF₆ interactions. The derived lattice constants and atomic coordinates depend only on the ratio of A to B and not on the individual magnitudes.

Atom pair	(A/B) (Å ⁶)	C (Å ⁻¹)
F ··· F	0.01517	3.60
F ··· S	0.03374	3.22
S ··· S	0.07503	2.84

To investigate the effectiveness of the new procedure in avoiding false minima, we arbitrarily selected three distinctly different false minima from the large number of solutions that were generated by a more conventional refinement procedure with the data at 23 K. Lattice constants differed from those cited above by as much as 2.1 Å and 6.9°. When these constants were introduced as starting parameters in the present procedure, all three smoothly refined to the solution tabulated above. Because the technique used to fit the data was based on adjustment of the entire pattern profile and was unconcerned with individual reflections as such, the overlapping of peaks introduced no difficulty. In fact, the approximately 40 peaks visible in Fig. 1 are composed of about 223 separate reflections. Each of the peaks shown is, on average, a superposition of six distinct reflections. It is therefore apparent why conventional indexing methods failed.

Subsequently, one of us (B.M.P.) investigated the pattern up to values of S of 2.5 Å⁻¹ at the highest resolution ($\lambda = 4.1037$ Å) for 23 K and, in a separate measurement,

extended the range of data to $S = 7.35$ Å⁻¹ ($\lambda = 1.48018$ Å) for $T = 23$ and 85 K. These extensive intensity data were subjected to a full Rietveld refinement (8). Such an analysis is a means of extracting from powder data, once the proper identification of reflections has been established, the positions and motions of the atoms within the unit cell. In favorable cases, its precision is comparable to that attainable in refinements of intensity data from single crystals. In the present case the Rietveld analysis (9) fully confirmed the correctness of the cell constants reported here.

The structure of the low-temperature phase of SF₆ has been resolved and it corresponds to that predicted by the molecular dynamics simulations (1). Although some uncertainties remain about the full range of conditions required for the stabilization of the intermediate trigonal phase, the theoretical modeling of the thermal properties of a prototype molecular solid is now almost complete. The method that made it possible to interpret the low-temperature powder pattern should be equally effective with

many other previously undecipherable diffraction patterns of materials that solidify only in a powdered form.

REFERENCES AND NOTES

1. G. S. Pawley and G. W. Thomas, *Phys. Rev. Lett.* **48**, 410 (1982).
2. G. S. Pawley and M. T. Dove, *Chem. Phys. Lett.* **99**, 45 (1983).
3. J. C. Taylor and A. B. Waugh, *J. Solid State Chem.* **18**, 241 (1976); G. Dolling, B. M. Powell, V. F. Sears, *Mol. Phys.* **37**, 1859 (1979).
4. G. Raynerd, G. J. Tatlock, J. A. Venables, *Acta Crystallogr.* **B38**, 1896 (1979).
5. L. S. Bartell, E. J. Valente, J. C. Caillat, *J. Phys. Chem.*, in press.
6. J. C. Caillat and L. S. Bartell, *Quantum Chemistry Program Exchange* (Program 520, Indiana University, Bloomington, IN, 1986).
7. D. E. Williams, *Quantum Chemistry Program Exchange* (Program 373, Indiana University, Bloomington, IN, 1979).
8. H. M. Rietveld, *J. Appl. Crystallogr.* **2**, 65 (1969). The Rietveld analysis can only succeed if the cell is quite well established at the outset. If the cell dimensions are unknown, the Rietveld method is as vulnerable to entrapment in false minima as any other standard method.
9. B. M. Powell *et al.*, in preparation.
10. Research at the University of Michigan was supported by a grant from the National Science Foundation. We thank G. S. Pawley for his helpful cooperation and L. Harsanyi for assistance in structural refinements that started from false solutions.

20 January 1987; accepted 14 April 1987

Frequency Dependence of Electric Field Modulation of Fibroblast Protein Synthesis

KENNETH J. MCLEOD,* RAPHAEL C. LEE, H. PAUL EHRLICH

The effect of electric current on protein biosynthesis in mammalian fibroblasts was investigated with neonatal bovine fibroblast-populated collagen matrices. The field strength dependence of electric field modulation of proline incorporation into extracellular and intracellular protein was measured over a frequency range from 0.1 to 1000 hertz. A frequency- and amplitude-dependent reduction in the rate of incorporation was observed. In tissues containing cells aligned either parallel or perpendicular to the electric field, this response was dependent on the orientation of the cells relative to the direction of the applied electric field. This study demonstrates that currents of physiological strength can stimulate alterations in biosynthesis and thereby may influence tissue growth, remodeling, and repair.

CELLS WITHIN MAMMALIAN connective and skeletal tissues are regularly exposed to time-varying electric currents. These currents are produced endogenously, arising predominantly from the spatial and temporal integration of currents from excitable cells (1), and through cur-

rents generated by mechanical strain in glycosaminoglycan-rich connective tissues (2) and bone (3). These currents may well regulate the growth and remodeling of tissues (4) and alter cellular function.

Physiological electric currents (5) can modulate the behavior of nonexcitable cells. For example, the rate of DNA synthesis by pelleted chondrocytes was enhanced by applied current densities of less than 10 μA/cm² (6). Glycosaminoglycan synthesis by chondrocytes in monolayer culture was enhanced by current densities as low as 1 μA/cm² (7). In organ culture, current densities of 1 to 5 μA/cm² have been shown to alter calcium metabolism in chick tibiae (8).

We have measured the rate of incorpo-

ration of proline into protein by bovine fibroblasts cultured within collagen matrices and found that it is sensitive to sinusoidal electric currents in the frequency range from 0.1 to 1000 Hz. This response manifests an abrupt current density threshold that is frequency-dependent. In addition, we found this threshold of the current density to be dependent on the orientation of the cell with respect to the direction of the applied current.

The remodeling of connective tissue is regulated by physical stresses (9). Because fibroblasts are primarily responsible for this remodeling in soft connective tissue, they were selected for these experiments. Neonatal bovine fibroblasts were obtained by disaggregating superficial fascial tissue from the thigh of 2-week-old calves by serial trypsin and collagenase digestions. The cells obtained were plated in flasks, maintained in Dulbecco's modified Eagle's medium (DMEM) containing 10% calf serum, and transferred to new flasks to avoid overcrowding two to five times prior to incorporation into gels.

To control the extracellular matrix composition and cell density, we fabricated tissues of constant composition by incorporating fibroblasts in collagen matrices using the technique of Bell *et al.* (10). Native type I collagen (2 mg/ml) was obtained through extraction of the tail tendons of young (less than 2 months old) Sprague-Dawley rats

K. J. McLeod and R. C. Lee, Continuum Electromechanics Group, Laboratory for Electromagnetic and Electronic Systems, Department of Electrical Engineering and Computer Science, Massachusetts Institute of Technology, Cambridge, MA 02139.
H. P. Ehrlich, Shriner's Burns Institute, Massachusetts General Hospital, Boston, MA 02139.

*Present address: Department of Orthopaedic Surgery, State University of New York, Health Sciences Center, Stony Brook, NY 11790.